Ultrasonics 54 (2014) 1015–1019

Contents lists available at ScienceDirect

Ultrasonics

journal homepage: www.elsevier.com/locate/ultras

Ultrasonic assembly of anisotropic short fibre reinforced composites

M.-S. Scholz [a,*], B.W. Drinkwater [b], R.S. Trask [a]

[a] Advanced Composites Centre for Innovation and Science (ACCIS), University of Bristol, Queen's Building, University Walk, Bristol BS8 1TR, United Kingdom
[b] Department of Mechanical Engineering, University of Bristol, Queen's Building, University Walk, Bristol BS8 1TR, United Kingdom

ARTICLE INFO

Article history:
Received 28 October 2013
Received in revised form 29 November 2013
Accepted 2 December 2013
Available online 9 December 2013

Keywords:
Discontinuous fibre composites
Mechanical properties
Acoustic radiation pressure
Particle manipulation

ABSTRACT

We report the successful manufacture of short fibre reinforced polymer composites via the process of ultrasonic assembly. An ultrasonic device is developed allowing the manufacture of thin layers of anisotropic composite material. Strands of unidirectional reinforcement are, in response to the acoustic radiation force, shown to form inside various matrix media. The technique proves suitable for both photo-initiator and temperature controlled polymerisation mechanisms. A series of glass fibre reinforced composite samples constructed in this way are subjected to tensile loading and the stress–strain response is characterised. Structural anisotropy is clearly demonstrated, together with a 43% difference in failure stress between principal directions. The average stiffnesses of samples strained along the direction of fibre reinforcement and transversely across it were 17.66 ± 0.63 MPa and 16.36 ± 0.48 MPa, respectively.

1. Introduction

Acoustic levitation techniques have been widely studied within the biological and medical disciplines, primarily to manipulate cells and molecules whose size range lies outside the capabilities of optical tweezers. Since, ultrasonic assembly has been applied more widely, with the trapping of micron to millimetre size objects of different shapes and sizes, and the formation of ordered arrays of particles having become possible. Recently, a number of authors have reported the successful casting of ultrasonically arranged particles inside various matrix media; these include acrylics, agar, epoxy, polyester and also polysiloxane [1–6]. However, to date little is known about the structural performance of ultrasonically formed materials. In this study we explore the feasibility of employing ultrasonic assembly to enable the manufacture of structurally efficient discontinuous fibre (short fibre) composites. Specifically, the fabrication of single layers of glass fibre reinforced polymers is presented, and an investigation is made into the mechanical properties of these laminar two-phase materials. The aim is to demonstrate that ultrasonic assembly is a credible tool for the manufacture of engineering materials.

Discontinuous fibre composites have lately re-gained interest, for use within additive layer manufacturing technologies. In particular, the effective placement and alignment of reinforcement entities are presently the focus of research attention. Although alignment of fibres can be achieved using electric or magnetic fields, these generally only allow for nematic phases to be formed [7,8]. In contrast, recent developments in the field of ultrasonics have shown that nano to millimetre size particles can be arranged into various patterns across all three spatial dimensions by acoustic standing waves [9–11]. Here, an acoustic pressure gradient causes a radiation force to be exerted on arbitrarily shaped objects drawing them towards either pressure nodes or pressure anti-nodes, depending on the relative density of particle to suspending fluid.

One of four distinct approaches may currently be taken to generate patterns of acoustic radiation forces: mode switching [12], focused ultrasonic beams [13,14], linear arrays of transducers facing a reflective surface [15–17], and the emission of counter-propagating travelling waves [18–20]. Here, counter-propagating devices are considered as they are relatively less sensitive to changes in the resonant frequency of the chamber due to the presence of large numbers of fibrous entities [20,21]. Further, nodal positions are not fixed by the geometry but by altering the relative phase of the counter-propagating waves, particles can be moved within the chamber [19,20].

While little is known theoretically about the effect of ultrasound on dense distributions of fibrous entities and fibre agglomerates, acoustic radiation forces on single cylindrical particle geometries have been extensively studied [22–33]. Specifically, the forces on rigid, elastic, and viscoelastic cylinders have been evaluated across a range of frequencies. The direction of the incident radiation is hereby generally taken to be perpendicular to the cylinder's long axis, thus restricting any particle motion to one dimension.

With ultrasonic assembly techniques allowing both the alignment and positioning of individual particles, additional control may be gained over discontinuous reinforcement distributions. A wide variety of fibre architectures may, in principle, be generated, hence improving the performance and structural efficiency of short fibre filled materials. To take one example, a composite's susceptibility to impact damage, wear, longitudinal micro-buckling,

* Corresponding author. Tel.: +44 1173315504.
E-mail address: M.Scholz@bristol.ac.uk (M.-S. Scholz).

0041-624X/$ - see front matter © 2014 Elsevier B.V. All rights reserved.
http://dx.doi.org/10.1016/j.ultras.2013.12.001

delamination, and fatigue is thought to be decreased as a result of in-plane and out-of-plane reinforcement, i.e. engineered reinforcement across all three spatial dimensions [7].

Similarly, no means are currently available for the additive layer processing of fibre reinforced polymer composites. Here, difficulties arise from the use of continuous fibre strands, again strongly indicating the need for structurally improved discontinuous fibre composites.

In the present article, the manufacture of thin layer discontinuous fibre composites via ultrasonic assembly techniques is demonstrated. Firstly, relevant material phases and experimental structures are introduced. A description of the ultrasonic assembly process follows, together with an outline of how suitable composite samples are fabricated for mechanical testing. Finally, the structural characteristics of test specimens are investigated, specifically looking to observe anisotropic behaviour.

2. Experimental methods and results

2.1. Materials

The blend of fibre composite material used was based on the aromatic dimethacrylate monomer 2,2-bis[p-(2-hydroxy-3-methacryloxypropoxy)phenyl]propane (BisGMA), a foundation commonly used for dental composite applications. To lower the viscosity of the bulky BisGMA monomer (from $\eta_{BisGMA} \approx 800$ Pa s to $\eta_{resin} \approx 0.76$ Pa s [34]), it was mixed with the comonomer triethylene glycol dimethacrylate (TEGDMA) in a ratio of 1:1 by weight. 0.2 wt% of camphorquinone (CQ) and 0.8 wt% of ethyl 4-(dimethylamino)benzoate (EDB) were also added to achieve radical photo-polymerisation at a wavelength of 460 nm. Complete ploymerisation was reached following exposure to a 900 mW light-emitting diode (LED) for approximately 40 s.

Commercially available, milled glass fibres (Lanxess MF7904) were used as reinforcement, with a nominal length of 50 μm and approximately 14 μm in diameter.

Note that in Section 2.3, the ultrasonic assembly of glass particles into lines of unidirectional reinforcement is also shown across a range of other matrix media including agar, silicone, and polyester resins.

2.2. Experimental setup

A schematic depicting the experimental setup is shown in Fig. 1. Counter-propagating waves are generated by two opposing $0.975 \times 15 \times 2$ mm lead zirconate titanate (PZT) transducers, which together form a standing wave field inside the device's central cavity. To allow for both piezoceramic plates to be recycled post matrix polymerisation, a sacrificial poly(methyl methacrylate) (PMMA) boundary is introduced between the acoustic drivers and the resin. The PMMA frame is mounted on a glass substrate using adhesive tape (tesa 64621-00007-01), and allows for easy optical access. Two further chambers on either side of the device are filled with water, providing a necessary heat sink at high driving voltages. Each transducer is held in place by a spring, gently pressing it against the PMMA boundary layer. The dimensions of the central cavity are $30 \times 15 \times 2$ mm, suitably large to manufacture samples for mechanical testing but allowing the driving voltage to be kept at 80 V_{pp}; an operation at relatively low voltages is desirable primarily to minimise the effects of acoustic streaming inside the central cavity. In the x–y plane the sample size was constrained to the dimensions of the device cavity, the thickness (z-direction) could be controlled by varying the amount of resin added.

To evaluate the acoustic properties of the present system, a one-dimensional electro-acoustic transmission line model [35] was used. The model assumes linear wave propagation through a series of passive layers of material, infinite in the directions perpendicular to the direction of propagation. An equivalent circuit approach [36] is taken to represent the electrically active piezoelectric plates. A detailed description of these methods is given in an article by Wilcox et al. [37]. Using this model, the first three resonances of the transducer are calculated to be: 2.01 MHz, 6.77 MHz, and 11.00 MHz. Here, we limit operation to the first of these frequencies, which we predict to maximise acoustic pressure for a given applied voltage. Specifically, the acoustic pressure inside the central cavity is estimated to be 1.2 MPa at a frequency, $f = 2.01$ MHz, a driving voltage, $V = 80$ V_{pp}, and taking an epoxy resin as an example. For the same scenario, the forces acting on a fluid suspended spherical glass particle ($r = 25$ μm) are calculated using the approach of Gor'kov [38], to be of the order of 34 nN.

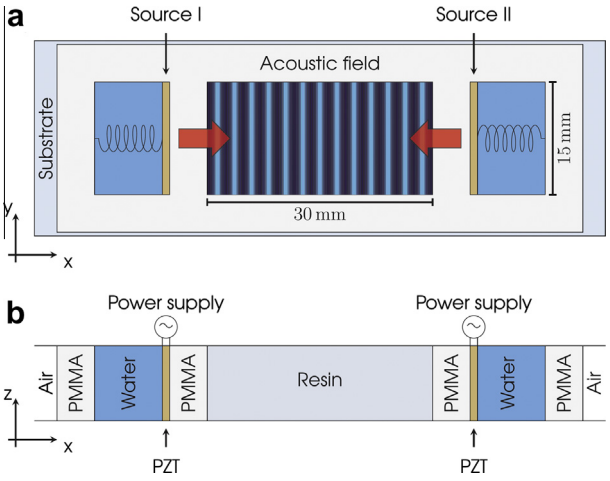

Fig. 1. Ultrasonic device. (a) A standing wave acoustic field is formed inside a central fluid volume, by interference of two counter-propagating traveling waves. The PZT transducers are submerged in water for cooling purposes, and held in place by small compression springs. (b) A device representation by material layers: air (∞), PMMA (5 mm), H_2O (9.025 mm), PZT (0.975 mm), PMMA (5 mm), resin (30 mm), PMMA (5 mm), PZT (0.975 mm), H_2O (9.025 mm), PMMA (5 mm), air (∞).

The composite assembly time is critically dependent on viscosity, with the fluid drag constituting the dominant resistive force to any particle motion. A low viscosity resin is thus generally preferred. For short glass fibres ($r \leqslant 25$ μm) dispersed in water ($\eta_{water} \approx 0.8e{-}3$ Pa s), full assembly is experimentally achieved in less than 100 ms, with particles traveling to pressure nodes. Given a linear dependency of the drag force on viscosity, an equivalent assembly time of 950 ms is calculated for fibres suspended in the resin.

2.3. Ultrasonic assembly

Representative micrographs of milled glass fibres assembled into lines of unidirectional reinforcement are shown in Fig. 2(a–d). Note, the separation of the lines varies with wavelength in the matrix material. A typical sample cross-section, produced by X-ray micro-tomography (μCT), can be seen in Fig. 2(e).

A range of matrix materials has been used to demonstrate the versatility of the ultrasonic assembly mechanism. While both agar and silicone materials relied on a temperature dependent polymerisation mechanism, a photo-initiator system was used to cure polyester and epoxy samples. Varying degrees of alignment are achieved, depending on the volumetric ratio of fibre to host media. For low fibre volume fractions, more distinct line features can be achieved, with individual particles generally being well aligned. High fibre volume fractions lead to the formation of long parallel strands of reinforcement with a higher degree of misalignment present within each line.

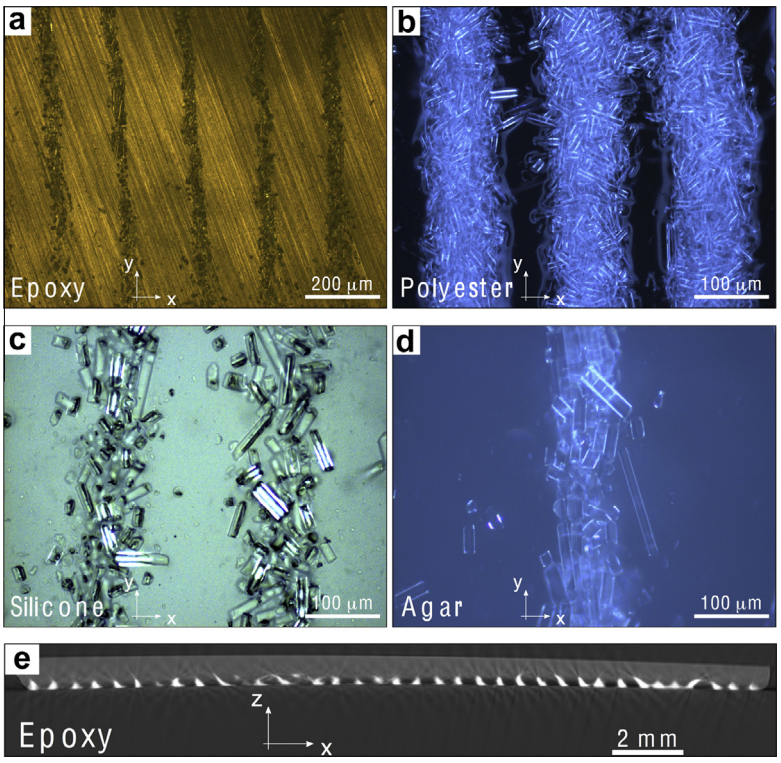

Fig. 2. Ultrasonic assembly of glass particles into lines of unidirectional reinforcement in (a) epoxy (c = 1510 m s^{-1} ± 2.8%), (b) polyester (c = 1347 m s^{-1} ± 2.5%), (c) silicone (c = 1070 m s^{-1} ± 4.4%), (d) agar (c = 1513 m s^{-1} ± 2.9%). Examples are shown at different magnifications and for varying fibre volume fractions. A typical sample cross-section (e) is presented in the form of a X-ray micro-tomography image. Fibre lines extend along the y-direction and are separated in the x-direction by a theoretical distance of $\lambda/2 = c/2f$, where c is the speed of sound in the matrix material and f is the driving frequency.

2.4. Fabrication of mechanical test specimens

The fabrication process for the ultrasonically assembled samples, is shown diagrammatically in Fig. 3. Firstly, some dry fibre reinforcements were distributed on the substrate. About 0.8 ml of resin was then added, before the two phases were mixed to give an even dispersion of glass particles on the bottom surface. An ultrasonic field was applied to drive the fibres to the nodal positions of the resulting standing wave. Given a driving frequency of 2.01 MHz and assuming a speed of sound, c = 1480 m s^{-1} in the fluid, lines of fibres are predicted to form at a separation of $\lambda/2 = 368$ μm, where λ is the acoustic wavelength; experimental measures find this separation to be in the range 350–380 μm. Prior to polymerisation initiation, reinforcement entities were allowed approximately 60 s to arrange and orient themselves under the influence of ultrasound. Finally, the resin was exposed to a blue light LED and cured in 40 s. No geometrical changes (such as narrowing or broadening of the lines) were observed during the rapid solidification phase.

Following the removal of the acoustic drivers and the substrate, two identical 13.6 × 13.6 mm test pieces were cut from the original sample using a high precision CO_2 laser. Across samples, the fibre volume fraction, V_f was estimated to be 9.0 ± 2.0%, by μCT analysis; for each pair of test pieces, V_f was assumed to be the same. By means of the above procedure a true comparison of mechanical test results could be established for each pair of test pieces. An analysis between samples also serves to quantify general manufacture consistency, to estimate average strength and stiffness values, and to determine failure mechanisms. The slight meniscus formed by excess resin on top of each specimen was removed by abrading all specimens to a uniform thickness of 0.50 ± 0.05 mm. To allow for better gripping of the test pieces during mechanical testing (in tension), end tabs – as depicted in Fig. 4 – were attached to the specimens. A set each of randomly dispersed fibre samples and neat resin specimens were prepared in the same manner but no ultrasonic energy was applied in these cases.

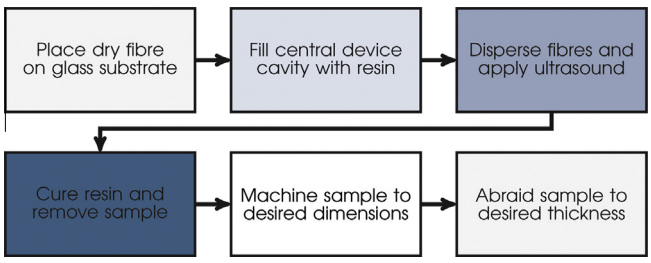

Fig. 3. Flow chart showing the sequence of the sample fabrication process.

2.5. Demonstration of structural anisotropy

The samples were mechanically tested in tension at a displacement controlled crosshead speed of 0.10 mm min^{-1}. The results are

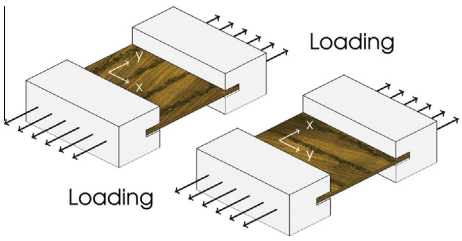

Fig. 4. Schematic illustration of the specimen geometry for mechanical characterisation. End tabs were adhered to each pair of test specimens. In one case end tabs were attached parallel to the direction of fibre reinforcement, in the other they were transversely oriented.

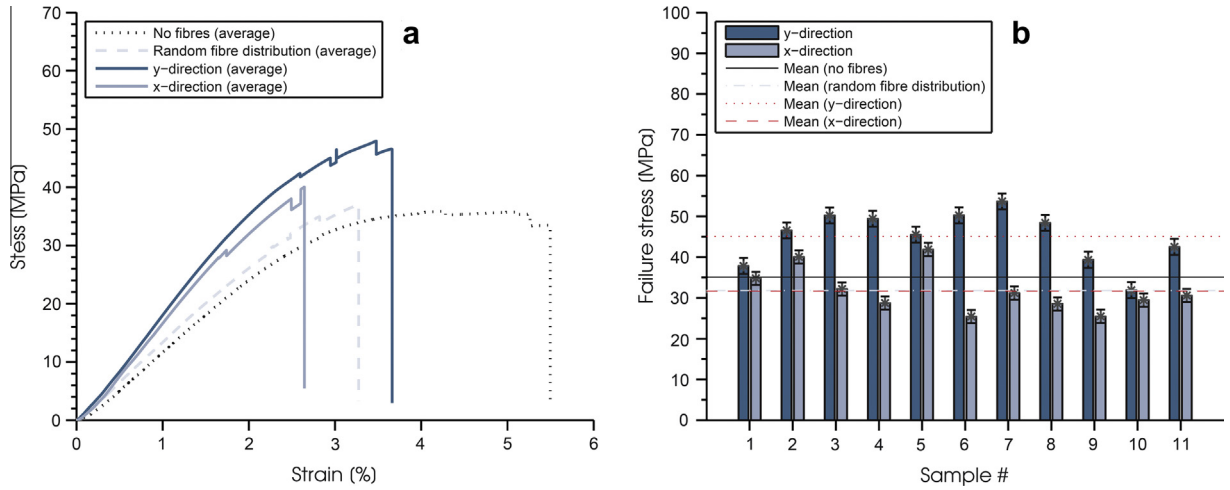

Fig. 5. Tensile test results for short glass fibre reinforced composite samples (with microstructure as per Fig. 2(a)). (a) The average stress–strain response is shown across samples without reinforcement, samples with randomly distributed reinforcement, samples reinforced in the *x*-direction, and samples whose reinforcement runs along the direction of loading. (b) A comparison of failure strength for the same set of test specimens.

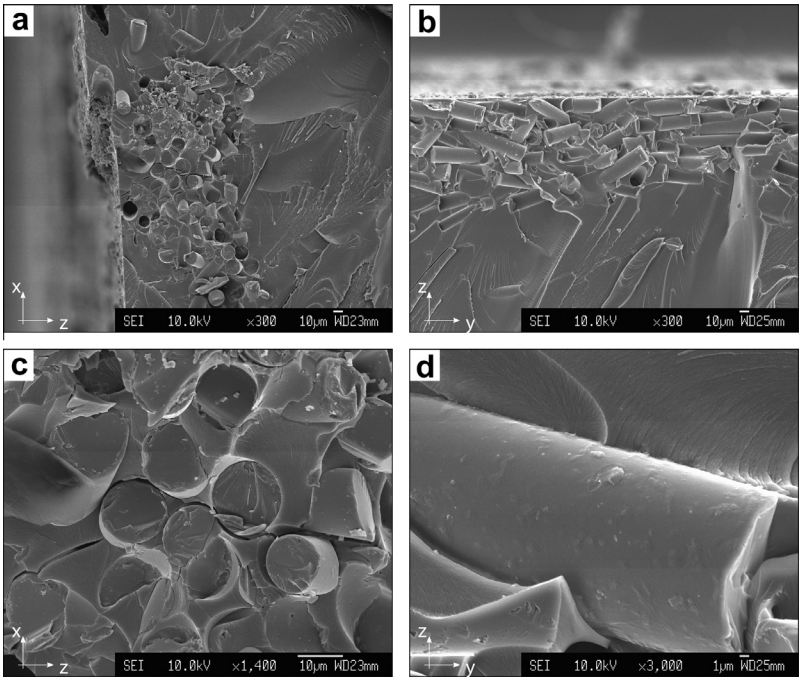

Fig. 6. SEM of the fracture surfaces, (a) for a sample subjected to loading in the *y*-direction, (b) a sample strained in the *x*-direction. Higher magnification images providing greater detail of the fracture surfaces in (a and b), are shown in (c and d), respectively.

summarised in an average stress vs. strain plot, shown in Fig. 5. A comparison of material strength along the line of fibre reinforcement (*y*-direction) with that across it (*x*-direction) is also given in the same figure.

An average stiffness of 16.36 ± 0.48 MPa was recorded for transversely strained samples; in comparison, specimens loaded in the direction of fibre reinforcement consistently showed superior mechanical performance with an average stiffness of 17.66 ± 0.63 MPa. The Young's modulus of samples without reinforcement and randomly oriented reinforcement were obtained as 11.51 ± 0.45 MPa and 13.33 ± 0.45 MPa, respectively. It is thus evident that improved structural properties and anisotropy have been achieved. On comparison between samples with randomly oriented reinforcements and ultrasonically assembled samples strained transversely, one notes that the latter appear to provide greater stiffness. We believe that this is due to the fact that within the assembled lines, fibres are in close proximity allowing interaction and load transfer, which results in increased stiffness. Within the random samples the fibres are dispersed and cannot interact.

As is clear from Fig. 5, the matrix itself exhibits a more ductile mechanical behaviour with strains to failure of up to 5.55 ± 0.30%; on the addition of fibre reinforcement, a more brittle failure mechanism is observed with failure generally occurring in a region of 2–3% strain.

For an estimation of the expected composite stiffness, E, the basic rule of mixtures (assuming continuous fibre reinforcement) was applied:

$$E = V_f E_f + (1 - V_f) E_m. \quad (1)$$

Here, E_m, and E_f are the Young's modulus of the matrix and the fibres, respectively. Across all samples, an average $E = 18.97 \pm 1.50$ MPa was so calculated, taking $V_f = 9.0 \pm 2.0\%$ as previously

obtained from μCT analysis (Fig. 2(e)), which is in good agreement with that measured experimentally.

To gain an understanding of the failure mechanism, scanning electron microscopy (SEM) was employed and the fracture surfaces of the samples were inspected (Fig. 6). A good degree of fibre alignment can be seen for both samples loaded in the *y*- (Fig. 6(a)) and *x*-direction (Fig. 6(b)). Some fibre pullout, and cracks running along the sample *z*-direction are indicative of failure due to loading in the *y*-direction (Fig. 6(c)). At high magnifications (Fig. 6(d)), good adhesion between the reinforcements and the surrounding matrix is apparent, while large amounts of matrix deformation can also be observed; this is evident particularly for samples loaded in the *x*-direction.

3. Conclusions

In summary, ultrasonic particle manipulation techniques were used to manufacture thin, single layers of short glass fibre reinforced polymer composites. A new type of ultrasonic device was developed, separating the acoustic system from the resin cavity to allow for the easy manufacture of multiple samples. Further, an effective method has been outlined to manufacture and mechanically characterise these thin laminar two-phase materials. With an 8% difference in stiffness between the two principal directions, anisotropy was demonstrated for unidirectionally reinforced discontinuous fibre composites under uniaxial tensile loading. A 43% improvement in strength could be observed for samples tested along the direction of fibre reinforcement over those strained perpendicular to the fibre direction, despite the relatively low volume percentage of the reinforcement phase.

With acoustic assembly techniques able to generate a wider range of fibre architectures, the realisation of both in- and out-of-plane reinforcement may in the future also become possible. Besides, ultrasonic assembly methodologies hold the potential to be used as part of an additive layer fabrication process, thus enabling the rapid prototyping manufacture of structurally efficient short fibre composites.

Acknowledgments

The authors gratefully acknowledge funding from the EPSRC as part of the Sonotweezers project (Grant No. EP/G012067/1), and under its ACCIS Doctoral Training Centre grant (Grant No. EP/G036772/1). Further support was received from the Bristol Centre for Nanoscience and Quantum Information (NSQI).

References

[1] M. Saito, T. Daian, K. Hayashi, S.-Y. Izumida, Fabrication of a polymer composite with periodic structure by the use of ultrasonic waves, J. Appl. Phys. 83 (1998) 3490–3494.
[2] M. Saito, Y. Imanishi, Host–guest composites containing ultrasonically arranged particles, J. Mater. Sci. 35 (2000) 2373–2377.
[3] Y. Cao, W. Xie, J. Sun, B. Wei, S. Lin, Preparation of epoxy blends with nanoparticles by acoustic levitation technique, J. Appl. Polym. Sci. 86 (2002) 84–89.
[4] L. Gherardini, C. Cousins, J. Hawkes, J. Spengler, S. Radel, H. Lawler, B. Devcic-Kuhar, M. Gröschl, W. Coakley, A. McLoughlin, A new immobilisation method to arrange particles in a gel matrix by ultrasound standing waves, Ultrasound Med. Biol. 31 (2005) 261–272.
[5] F. Mitri, F. Garzon, D. Sinha, Characterization of acoustically engineered polymer nanocomposite metamaterials using X-ray microcomputed tomography, Rev. Sci. Instrum. 82 (2011).
[6] T. Tuziuti, Y. Masuda, K. Yasui, K. Kato, Two-dimensional patterning of inorganic particles in resin using ultrasound-induced plate vibration, Jpn. J. Appl. Phys. 50 (2011) 088006.
[7] R. Erb, R. Libanori, N. Rothfuchs, A. Studart, Composites reinforced in three dimensions by using low magnetic fields, Science 335 (2012) 199–204.
[8] C. Park, J. Wilkinson, S. Banda, Z. Ounaie, K. Wise, G. Sauti, P. Lillehe, J. Harrison, Aligned single-wall carbon nanotube polymer composites using an electric field, J. Polym. Sci. Part B: Polym. Phys. 44 (2006) 1751–1762.
[9] S. Yamahira, S. Hatanaka, M. Kuwabara, S. Asai, Orientation of fibers in liquid by ultrasonic standing waves, Jpn. J. Appl. Phys. 39 (2000) 3683–3687.
[10] L. Kuznetsova, D. Bazou, G. Edwards, W. Coakley, Multiple three-dimensional mammalian cell aggregates formed away from solid substrata in ultrasound standing waves, Biotechnol. Prog. 25 (2009) 834–841.
[11] B. Raeymaekers, C. Pantea, D. Sinha, Manipulation of diamond nanoparticles using bulk acoustic waves, J. Appl. Phys. 109 (2011) 014317.
[12] P. Glynne-Jones, R. Boltryk, N. Harris, A. Cranny, M. Hill, Mode-switching: a new technique for electronically varying the agglomeration position in an acoustic particle manipulator, Ultrasonics 50 (2010) 68–75.
[13] J. Wu, G. Du, Acoustic radiation force on a small compressible sphere in a focused beam, J. Acoust. Soc. Am. 87 (1990) 997–1003.
[14] J. Lee, S.-Y. Teh, A. Lee, H. Kim, C. Lee, K. Shung, Single beam acoustic trapping, Appl. Phys. Lett. 95 (2009) 073701.
[15] T. Kozuka, T. Tuziuti, H. Mitome, T. Fukuda, Acoustic micromanipulation using a multi-electrode transducer, in: Proceedings of the Seventh International Symposium on Micro Machine and Human Science, 1996, pp. 163–170.
[16] T. Kozuka, T. Tuziuti, H. Mitome, T. Fukuda, Control of a standing wave field using a line-focused transducer for two-dimensional manipulation of particles, Jpn. J. Appl. Phys. 37 (1998) 2974–2978.
[17] P. Glynne-Jones, C. Démoré, C. Ye, Y. Qiu, S. Cochran, M. Hill, Array-controlled ultrasonic manipulation of particles in planar acoustic resonator, IEEE Trans. Ultrason., Ferroelectr., Freq. Control 59 (2012) 1258–1266.
[18] T. Kozuka, T. Tuziuti, H. Mitome, T. Fukuda, F. Arai, Control of position of a particle using a standing wave field generated by crossing sound beams, in: Proceedings of the 1998 IEEE Ultrasonics Symposium, vol. 1, 1988, pp. 657–660.
[19] C. Courtney, C.-K. Ong, B. Drinkwater, P. Wilcox, C. Demore, S. Cochran, P. Glynne-Jones, M. Hill, Manipulation of microparticles using phase-controllable ultrasonic standing waves, J. Acoust. Soc. Am. 128 (2010) EL195–EL199.
[20] C. Courtney, C. Ong, B. Drinkwater, A. Bernassau, P. Wilcox, D. Cumming, Manipulation of particles in two dimensions using phase controllable ultrasonic standing waves, Proc. R. Soc. A: Math., Phys. Eng. Sci. (2011).
[21] C. Kwiatkowski, P. Marston, Resonator frequency shift due to ultrasonically induced microparticle migration in an aqueous suspension: observations and model for the maximum frequency shift, J. Acoust. Soc. Am. 103 (1998) 3290–3300.
[22] J.W. Miles, Motion of a rigid cylinder due to a plane elastic wave, J. Acoust. Soc. Am. 32 (1960) 1656–1659.
[23] T. Hasegawa, K. Saka, N. Inoue, K. Matsuzawa, Acoustic radiation force experienced by a solid cylinder in a plane progressive sound field, J. Acoust. Soc. Am. 83 (1988) 1770–1775.
[24] P. Brodeur, J. Dion, J. Garceau, G. Pelletier, D. Massicotte, Fiber characterization in a stationary ultrasonic field, IEEE Trans. Ultrason., Ferroelectr., Freq. Control 36 (1989) 549–553.
[25] J. Wu, G. Du, S.S. Work, D.M. Warshaw, Acoustic radiation pressure on a rigid cylinder: an analytical theory and experiments, J. Acoust. Soc. Am. 87 (1990) 581–586.
[26] P. Brodeur, Motion of fluid-suspended fibres in a standing wave field, Ultrasonics 29 (1991) 302–307.
[27] W. Wei, D.B. Thiessen, P.L. Marston, Acoustic radiation force on a compressible cylinder in a standing wave, J. Acoust. Soc. Am. 116 (2004) 201–208.
[28] D. Haydock, Calculation of the radiation force on a cylinder in a standing wave acoustic field, J. Phys. A: Math. Gen. 38 (2005) 3279.
[29] F.G. Mitri, Radiation force acting on an absorbing cylinder placed in an incident plane progressive acoustic field, J. Sound Vib. 284 (2005) 494–502.
[30] F.G. Mitri, Frequency dependence of the acoustic radiation force acting on absorbing cylindrical shells, Ultrasonics 43 (2005) 271–277.
[31] F.G. Mitri, S. Chen, Theory of dynamic acoustic radiation force experienced by solid cylinders, Phys. Rev. E 71 (2005) 016306.
[32] F.G. Mitri, Z.E.A. Fellah, Acoustic radiation force on coated cylinders in plane progressive waves, J. Sound Vib. 308 (2007) 190–200.
[33] J. Wang, J. Dual, Theoretical and numerical calculation of the acoustic radiation force acting on a circular rigid cylinder near a flat wall in a standing wave excitation in an ideal fluid, Ultrasonics 52 (2012) 325–332.
[34] F. Gonalves, Y. Kawano, C. Pfeifer, J. Stansbury, R. Braga, Influence of BisGMA, TEGDMA, and BisEMA contents on viscosity, conversion, and flexural strength of experimental resins and composites, Eur. J. Oral Sci. 117 (2009) 442–446.
[35] M. Hill, The selection of layer thicknesses to control acoustic radiation force profiles in layered resonators, J. Acoust. Soc. Am. 114 (2003) 2654–2661.
[36] D. Leedom, R. Krimholtz, G. Matthaei, Equivalent circuits for transducers having arbitrary even- or odd-symmetry piezoelectric excitation, IEEE Trans. Son. Ultrason. 18 (1971) 128–141.
[37] P. Wilcox, R. Monkhouse, P. Cawley, M. Lowe, B. Auld, Development of a computer model for an ultrasonic polymer film transducer system, NDT & E Int. 31 (1998) 51–64.
[38] L.P. Gor'kov, On the forces acting on a small particle in an acoustical field in an ideal fluid, Sov. Phys. Dokl. 6 (1962) 773.